

This is the accepted manuscript made available via CHORUS. The article has been published as:

# Continuous and discontinuous dark solitons in polariton condensates

Stavros Komineas, Stephen P. Shipman, and Stephanos Venakides

Phys. Rev. B **91**, 134503 — Published 9 April 2015

DOI: [10.1103/PhysRevB.91.134503](https://doi.org/10.1103/PhysRevB.91.134503)

# Continuous and discontinuous dark solitons in polariton condensates

Stavros Komineas,<sup>1</sup> Stephen P. Shipman,<sup>2</sup> and Stephanos Venakides<sup>3</sup>

<sup>1</sup>*Department of Mathematics and Applied Mathematics,  
University of Crete, 71003 Heraklion, Crete, Greece*

<sup>2</sup>*Department of Mathematics, Louisiana State University, Baton Rouge, Louisiana 70803, USA*

<sup>3</sup>*Department of Mathematics, Duke University, Durham, North Carolina 27708, USA*

Bose-Einstein condensates of exciton-polaritons are described by a Schrödinger system of two equations. Nonlinearity due to exciton interactions gives rise to a frequency band of dark soliton solutions, which are found analytically for the lossless zero-velocity case. The soliton's far-field value varies from zero to infinity as the operating frequency varies across the band. For positive detuning (photon frequency higher than exciton frequency), the exciton wavefunction becomes discontinuous when the operating frequency exceeds the exciton frequency. This phenomenon lies outside the parameter regime of validity of the Gross-Pitaevskii (GP) model. Within its regime of validity, we give a derivation of a single-mode GP model from the initial Schrödinger system and compare the continuous polariton solitons and GP solitons using the healing length notion.

## I. INTRODUCTION

Exciton-polaritons are matter-light quasiparticles that arise from the coupling between excitons and photon modes in a semiconductor microcavity and can form Bose-Einstein condensates (BEC) at relatively high temperatures [1–4]. Polariton condensates are sustained by laser pumping of photons in a two-dimensional quantum well. In a mean-field approximation, their wavefunctions produce a rich variety of localised quantum states in the micrometer scale: dark solitons [5–8, 10], bright solitons [5, 11–13], vortices [14, 15]. Solitons in polaritonic condensates have potential for applications in ultrafast information processing [16] due to picosecond response times and strong nonlinearities [11, 12].

In this work, we report a frequency band of dark polariton solitons whose exciton wave function develops a discontinuity as the frequency is increased beyond the exciton frequency (Fig. 1). At the point of discontinuity, the photon field vanishes while the exciton field experiences a phase jump of  $\pi$ .

We investigate a one-dimensional condensate of polaritons in a strongly coupled exciton and photon system. Our derivation depends crucially on the use of the classic model that retains separate wave functions for the excitons and the photon modes, and thus illuminates phenomena outside the regime described by the Gross-Pitaevskii model. Exciton interactions are modelled by a nonlinear term, while photons are dispersive. Neglecting both pumping and losses (which are due to radiation and thermalization) and thus focusing on the synergy of exciton interaction (nonlinearity) and photon dispersion allows us to produce analytical formulae for polariton solitons. A remarkable property of the solitons we derive is that the operating frequency can be tuned to produce a far-field baseline amplitude ranging from 0 to an arbitrarily large value.

We use the term “soliton” (instead of solitary wave or localized structure) in the spirit of conforming to the prevailing language. The term “soliton” was coined in the

1960s to describe nonlinear solitary waves that interact cleanly (without radiating). Since then, the use of the term has been broadened, especially in the physics literature, to encompass more general localized wave forms.

Sec. II presents the derivation of dark solitons for the conservative polariton equations, Sec. III draws a comparison with the standard Gross-Pitaevskii model, Sec. IV contains a description of soliton solutions as bound states in a potential well, and Sec. V contains concluding remarks.

## II. POLARITON SOLITONS

We consider a one-dimensional semiconductor microcavity in which a photon field  $\psi_C(x, t)$  interacts with an exciton field  $\psi_X(x, t)$ . One dimensional or nearly one dimensional polariton structures have been observed in [6, 10, 17] and in [18] (for radial fields). The pair  $(\psi_X, \psi_C)$  is a polariton field and its dynamics are modeled by the system [1, 19–21]

$$i\partial_t\psi_X = (\omega_X + g|\psi_X|^2)\psi_X + \gamma\psi_C \quad (1a)$$

$$i\partial_t\psi_C = (\omega_C - \frac{1}{2}\partial_{xx})\psi_C + \gamma\psi_X. \quad (1b)$$

The coupling constant is half the Rabi frequency  $\gamma = \Omega_R/2$ ;  $\omega_X$  is the frequency of a free exciton, and  $\omega_C$  is the photon frequency at zero wavenumber. All these are normalized to a reference frequency  $\gamma_0$ . One could set  $\gamma_0 = \gamma$ , however, we prefer to keep  $\gamma$  as an explicit parameter. The spatial variable  $x$  is normalized to  $\ell_0 = \sqrt{\hbar/(\gamma_0 m_C)}$ , where  $m_C$  is the effective photon mass. The system of Eqs. (1) is conservative (it conserves energy and total number of particles: excitons and photons) as we have neglected losses. Losses are typically included by adding imaginary part to  $\omega_X$  and  $\omega_C$ .

The wavefunctions  $\psi_X, \psi_C$  are normalized to  $\sqrt{N_0}/\ell_0$ , where  $N_0$  is a reference number of particles. The nonlinearity parameter  $g$  is normalised to  $N_0/(\ell_0^2\gamma_0)$ . We consider only the case  $g > 0$  in this paper.

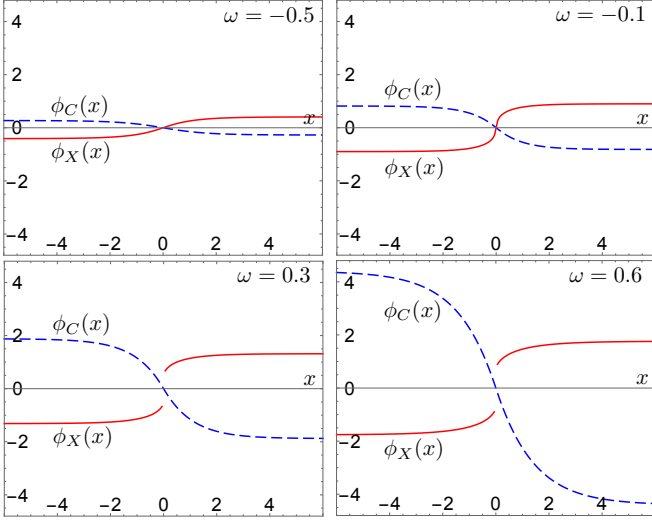


FIG. 1: Dark polariton soliton envelopes  $(\phi_X(x), \phi_C(x))$  for exciton frequency  $\omega_X = 0$  and photon frequency  $\omega_C = 1$ , which gives a threshold frequency  $\omega_{LP} \approx -0.618$  for the onset of the soliton, a transition frequency  $\omega_X = 0$  at which  $\phi_X$  becomes discontinuous, and a blowup frequency  $\omega_C = 1$  at which the far-field values of  $\phi_X$  and  $\phi_C$  become unbounded as shown in Fig. 3 (right). These graphs demonstrate the increasing soliton amplitude as  $\omega$  increases through four values. When  $\omega < \omega_X$ ,  $\phi_X$  is continuous, and when  $\omega > \omega_X$ ,  $\phi_X$  is discontinuous. The values of  $\phi_X$  and  $\phi_C$  are related by (4b).

We seek stationary harmonic polariton fields

$$\begin{aligned}\psi_X(x, t) &= \phi_X(x)e^{-i\omega t} \\ \psi_C(x, t) &= \phi_C(x)e^{-i\omega t}\end{aligned}\quad (2)$$

with operating frequency  $\omega$  and wavenumber zero. Letting

$$\varpi_X = \omega - \omega_X, \quad \varpi_C = \omega - \omega_C, \quad (3)$$

and inserting (2) into (1) yields

$$-\frac{1}{2}\phi_C'' - \varpi_C\phi_C + \gamma\phi_X = 0, \quad (4a)$$

$$\phi_C = \frac{1}{\gamma}(\varpi_X - g\phi_X^2)\phi_X. \quad (4b)$$

Multiplying Eq. (4a) by  $\phi_C'$  and Eq. (4b) by  $\gamma\phi_X'$  and adding the two integrates the system (4) exactly. The cubic algebraic relation (4b) allows one to eliminate  $\phi_C$  in favor of  $\phi_X$  to obtain a first-order ODE for  $\phi_X(x)$ . It is then convenient to use the scaled exciton density

$$\zeta(x) := g\phi_X(x)^2 \quad (5)$$

which eliminates  $g$  from the equation and results in

$$\frac{1}{2}\zeta'^2 = \frac{4\zeta Q(\zeta)}{(3\zeta - \varpi_X)^2}, \quad (6)$$

where  $Q(\zeta) = -\varpi_C[\zeta^3 - \frac{1}{2}(3\zeta_\infty + \varpi_X)\zeta^2 + \zeta_\infty\varpi_X\zeta + K]$ ,  $K$  is an arbitrary real constant of integration, and

$$\zeta_\infty = \varpi_X - \frac{\gamma^2}{\varpi_C} \quad (7)$$

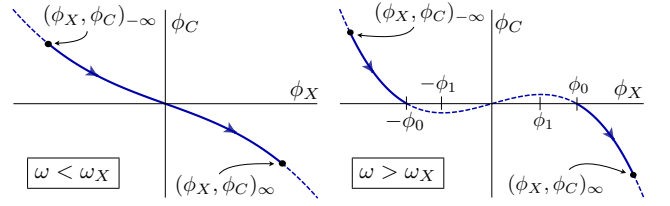


FIG. 2: The cubic relation (4b) giving the photon field envelope value  $\phi_C$  vs. the exciton field envelope value  $\phi_X$ . **Left.** The pair  $(\phi_X(x), \phi_C(x))$  travels continuously along the graph of the monotonic cubic between its far-field values as  $x$  increases from  $-\infty$  to  $\infty$ . **Right.** The pair jumps discontinuously between the points  $(-\phi_0, 0)$  and  $(+\phi_0, 0)$ , with  $\phi_0 = \sqrt{\varpi_X/g}$ . The transition from continuous to discontinuous  $\phi_X$  occurs when  $\omega = \omega_X$ . Graphs of the fields  $\phi_C(x)$  and  $\phi_X(x)$  are shown in Fig. 1. The singularity of the ODE (6) occurs at the critical points  $\pm\phi_1$ .

corresponds to the nonzero equilibrium solution of (4). Eq. (6) has the structure of an energy equation of a conservative system and admits a rich set of solitons and periodic structures. In this work, we focus on continuous and discontinuous dark solitons for  $g > 0$ .

For a dark soliton  $\zeta(x)$  to exist, the cubic polynomial  $Q(\zeta)$  must have a double root that serves as the soliton's far-field value. The value of the constant of integration  $K$  that provides such a nonzero double root equals

$$K = -\frac{\gamma^6}{2\varpi_C^3}(\eta - 1)^2, \quad (8)$$

where  $\eta$  is a convenient dimensionless parameter

$$\eta = \frac{\varpi_X\varpi_C}{\gamma^2}. \quad (9)$$

We calculate the double root to be equal to  $\zeta_\infty$ , given in (7). The fact that this is also the value of the far-field justifies the notation. As  $x$  is varied,  $\zeta(x)$  varies continuously down to its minimal value (nadir)  $\zeta = 0$ , which is a simple root of the potential in (6). We may assume that the nadir occurs at  $x = 0$ .

The soliton field  $(\phi_X(x), \phi_C(x))$  traces the graph of the cubic relation (4b) as  $x$  increases. Fig. 2 shows the graph of this relation for the two cases  $\omega < \omega_X$  and  $\omega > \omega_X$ . The equilibrium points  $(\phi_X, \phi_C)_\infty$  and  $(\phi_X, \phi_C)_\infty$  correspond to the calculated value  $\zeta_\infty$ .

The parameter  $\eta$  is convenient for expressing the soliton *nonlinear dispersion relation* at zero wavenumber, that relates the soliton amplitude  $\zeta_\infty$  to the operating frequency  $\omega$ , which is embodied in  $\eta$  and  $\varpi_C$ ,

$$\zeta_\infty = \varpi_X \frac{\eta - 1}{\eta} = \frac{\gamma^2}{\varpi_C}(\eta - 1). \quad (10)$$

We restrict our attention to  $\varpi_C < 0$ , which also implies  $\eta < 1$ , given the fact that  $\zeta_\infty > 0$ . Under these conditions, one can show that  $Q(\zeta) > 0$ , a necessary condition for Eq. (6) to have real solutions.

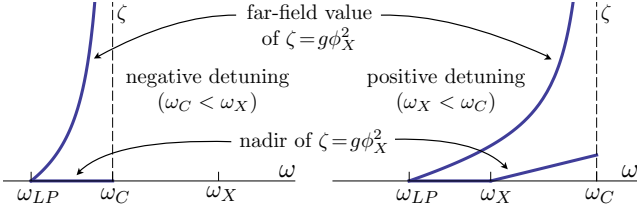


FIG. 3: The *threshold frequency*  $\omega_{LP}$  marks the onset of a dark polariton soliton, and the photon frequency  $\omega_C$  is the *blowup frequency*, at which the far-field amplitude of the soliton becomes unbounded. **Left.** ( $\omega_C < \omega_X$ ). As the operating frequency  $\omega$  traverses the soliton band ( $\omega_{LP}, \omega_C$ ), the far-field amplitude of the exciton field  $\phi_X$  goes from 0 to  $\infty$  according to (7). The nadir (low point) is zero. **Right.** ( $\omega_X < \omega_C$ ) The free exciton frequency  $\omega_X$  is the *transition frequency* from continuous to discontinuous solitons. The nadir of the discontinuous soliton is pushed upwards to the value  $\varpi_X$ .

A dark soliton appears at  $\eta = 1$  ( $\zeta_\infty = 0$ ) corresponding to a *threshold frequency*  $\omega_{LP}$ . This constitutes the linear limit of the soliton that emerges as the frequency increases; it is thus no surprise that the frequency  $\omega_{LP}$  coincides with the lower endpoint of the well-known lower band ( $\omega_{LP}, \omega_X$ ) of homogeneous linear ( $g = 0$ ) polaritons of the form  $(\phi_X, \phi_C)e^{i(kx - \omega t)}$ , with  $\phi_X$  and  $\phi_C$  constant [14];  $\omega_{LP}$  corresponds to  $k = 0$ . As the frequency is increased from its threshold, the amplitude of the soliton increases until it blows up at the photon frequency  $\omega_C$  ( $\eta = 0$ ,  $\zeta_\infty = \infty$ ). Fig. 3 displays the far-field and nadir values of the soliton *vs.* the frequency in the band from threshold to blowup, in the cases of negative detuning and positive detuning.

In the case of positive detuning,  $\omega_X < \omega_C$ , (*i.e.*  $\varpi_C < \varpi_X$ ), the frequency  $\omega_X$  lies within the soliton frequency band ( $\omega_{LP}, \omega_C$ ). This marks the *transition frequency* above which the soliton field  $\phi_X$  becomes discontinuous when the obstructing singularity  $\zeta = \varpi_X/3$  in (6) becomes positive, breaking into the soliton range  $[0, \zeta_\infty)$ . The nadir of the soliton is pushed upward from  $\zeta = 0$  to the value  $\zeta = \varpi_X$ , which is now positive, leading to a jump of the exciton field between the values  $\pm\phi_0 = \pm\sqrt{\varpi_X/g}$ . Fig. 2 traces the path of the pair  $(\phi_X(x), \phi_C(x))$  along the graph of the relation (4b) both for negative detuning and positive detuning. The system equations (4) remain valid, as the jump in  $\phi_X$  is balanced by a jump in  $\phi_C''$ . Physically, the photon field  $\phi_C$  which mediates the coupling between neighboring excitons through the term  $\gamma\phi_C$  in (1a), vanishes when  $\zeta$  takes the special value  $\varpi_X$  (corresponding to  $\phi_0 = \sqrt{\varpi_X/g}$  in Fig. 2b). The vanishing of the photon field turns off the coupling between neighboring excitons thus making the jump permissible. The formulae (7) and (10) for the far-field value  $\zeta_\infty$  remain the same.

Fig. 1 presents four instances of the soliton profile that show the progress towards the discontinuity (top) and the progress past the discontinuity of the exciton field (bottom). The photon field remains continuous. Its second

derivative has a discontinuity at  $x = 0$ , as discussed earlier, although this is too subtle to observe in the figure. Notice the monotonic increase of the far-field amplitude as the frequency  $\omega$  increases.

It is interesting to visualize the mechanism of the formation of the discontinuity of the exciton field  $\phi_X(x)$  by following the slope of this field at  $x = 0$ , as one lowers the dimensionless parameter  $\eta$  from its value  $\eta = 1$  at which the dark soliton is born. In order to calculate this slope, we express  $|\phi_X'(0)|$  in terms of  $\zeta$  and  $\zeta'$  from the relation  $\zeta = g\phi_X^2$ . We then insert the value for  $\zeta'$  from the differential equation (6) and, finally, set  $\zeta = 0$ . We obtain

$$[\phi_X'(0)]^2 = \frac{\gamma^2(\eta - 1)^2}{g\eta^2}. \quad (11)$$

For positive detuning and as  $\omega \nearrow \omega_X$ , the parameter  $\eta \searrow 0$  and thus, the slope  $\phi_X'(0)$  tends to infinity, while  $\phi_X$  remains finite. The jump discontinuity of the exciton envelope profile sets on as  $\eta$  becomes negative.

### III. HEALING LENGTH AND COMPARISON WITH GROSS-PITAEVSKII EQUATION

Adopting the slope of the profile at the origin  $x = 0$  as an indicator of the scale of the slope of the profile we define the *healing length* of a exciton field profile by

$$\xi_X = 2 \left| \frac{\phi_X(x = \pm\infty)}{\phi_X'(0)} \right|, \quad (12)$$

with a similar equation for the photon field. From the field envelope Eq. (4a), and the far-field Eq. (10), we obtain  $\phi_C(\infty)/\phi_X(\infty) = \gamma/\varpi_C$  and  $\phi_C'(0)/\phi_X'(0) = \varpi_X/\gamma$ . Thus, the healing lengths  $\xi_C$  and  $\xi_X$  are related by

$$\xi_C^2 = \frac{\xi_X^2}{\eta^2}. \quad (13)$$

Combining Eqs. (10), (11) and  $\zeta_\infty = g\phi_\infty^2$ , we obtain for the continuous soliton the healing lengths

$$\xi_X^2 = \frac{4\eta^2}{\varpi_C(\eta - 1)}, \quad \xi_C^2 = \frac{4}{\varpi_C(\eta - 1)}. \quad (14)$$

When  $\omega_C < \omega_X$ , near the blow-up frequency  $\varpi_C = 0$  ( $\eta = 0$ ) the healing length of the excitons approaches zero, while the photon healing length diverges to infinity. At the same time the far-field value goes to infinity. At the transition frequency  $\varpi_X = 0$  ( $\eta = 0$ ) (obtained only for positive detuning)  $\xi_X$  goes to zero linearly in  $\eta$  which one can view as a precursor to the discontinuity. The photon healing length converges to  $\xi_C^2 = 4/(\omega_C - \omega_X)$ . Fig. 1 exemplifies these observations.

In the region near the value  $\eta = 1$ , at which the continuous soliton begins its life, the exciton and the photon fields are nearly proportional to each other and  $\xi_C \approx \xi_X$ . The photon field is described well by a Gross-Pitaevskii

(GP) model that is derived as a simplification of the two-equation model (4). We solve Eq. (4b) for  $\phi_X$  as a power series in  $\phi_C$  up to the third degree term and we insert this value of  $\phi_X$  into Eq. (4a). There seems to be no analogous way to derive a GP equation for the exciton field. The GP model derived for the photon field is

$$\frac{1}{2}\phi'' - \varepsilon\varpi_C\phi - \tilde{g}\phi^3 = 0. \quad (15)$$

The notation  $\phi$  is a convenient abbreviation of the more descriptive notation  $\phi_{\text{GP,C}}$ . The parameter  $\varepsilon > 0$  measures the deviation from the linear problem and equals

$$\varepsilon = \frac{1 - \eta}{\eta}, \quad (16)$$

while  $\tilde{g} = (\frac{\varpi_C}{\varpi_X})^2 g$ .

Multiply by  $2\phi'$  and integrate to obtain

$$\frac{1}{2}\phi'^2 - \varepsilon\varpi_C\phi^2 - \frac{1}{2}\tilde{g}\phi^4 = E_0 \quad (17)$$

where  $E_0$  is a constant of integration. Like Eq. (6), this has the structure of a conservative system. The left side can be considered as the sum of a kinetic and a potential energy. It produces the GP approximation of the photon profile of the soliton we are investigating. The potential has two equal maxima at  $\pm\phi_\infty$  where

$$\phi_\infty^2 = -\frac{\varepsilon\varpi_C}{\tilde{g}}. \quad (18)$$

These are the far-field values ( $\phi' = 0$ ) for soliton solutions obtained from Eq. (17) at the peak of the potential

$$E_0 = -\varepsilon\varpi_C\phi_\infty^2 - \frac{1}{2}\tilde{g}\phi_\infty^4 = -\frac{1}{2}\varepsilon\varpi_C\phi_\infty^2. \quad (19)$$

We obtain from Eq. (17)  $\phi'(0)^2 = 2E_0 = -\varepsilon\varpi_C\phi_\infty^2$ . Taking, as before, the slope  $|\phi'(0)|$  as an indicator of the slope of the profile, the healing length for the photons is

$$(\xi_C^{\text{GP}})^2 = \frac{4\phi(\pm\infty)^2}{\phi'(0)^2} = \frac{4\phi_\infty^2}{\phi'(0)^2} = \frac{4\eta}{\varpi_C(\eta - 1)}. \quad (20)$$

The photon healing length for the approximate equation (GP) underestimates the healing length derived for the full system in (14) by a factor of  $\eta$ . The two agree at the linear limit  $\eta = 1$ .

#### IV. SOLITON AS A PHOTON FIELD IN A POTENTIAL WELL

Returning to the system involving both the photon and the exciton fields, one can write Eqs. (4) as a Schrödinger equation for the photon field envelope  $\phi_C$ ,

$$-\frac{1}{2}\phi_C'' + V(x)\phi_C = \varpi_C\phi_C, \quad (21)$$

in which the effective potential  $V(x)$  depends on the exciton field:

$$V(x) = \frac{\gamma^2}{\varpi_X - g\phi_X(x)^2}. \quad (22)$$

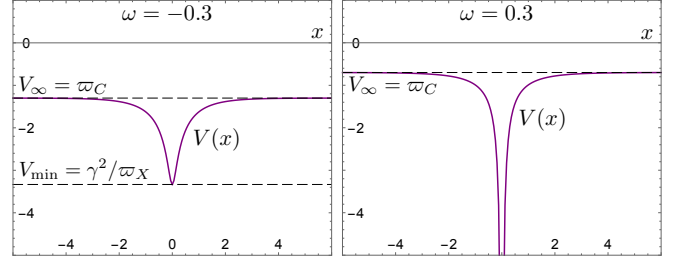


FIG. 4: The effective potential well  $V(x)$  that confines the photon field of an exciton-polariton soliton. **Left.** When the exciton field is continuous ( $\omega < \omega_X$ ),  $V(x)$  has a finite minimal value. **Right.** When the exciton field is discontinuous ( $\omega > \omega_X$ ),  $V(x)$  is unbounded at the point of discontinuity  $x = 0$ . ( $\omega_X = 0$ ,  $\omega_C = 1$ , and  $\omega_{\text{LP}} \approx -0.618$ , as in Fig. 1.)

For the dark soliton derived above,  $V(x)$  exhibits a single symmetric well with far-field value  $V_\infty = \varpi_C < 0$ , as shown in Fig. 4. For the continuous soliton,  $V$  has a minimal value of  $V_{\text{min}} = \gamma^2 / \varpi_X$ . For the discontinuous soliton, the well becomes infinitely deep at the point of discontinuity.

In an experimental setup, one expects that losses will allow some photons to be trapped by the potential well (22) in the form of bound states at discrete energy levels which lie below  $\varpi_C$ . As long as a small enough fraction of the energy of the photon field of the coherent polariton structure is transferred into lower energy states, the exciton field  $\phi_X(x)$  and therefore also the potential  $V(x)$  will not be significantly altered and can be considered a fixed potential.

This scenario is consistent with experimental observations [17], in which a polariton field is sustained by continuously injecting photons at two pump spots, one on each side of the potential well. A fraction of the polariton population descends to lower energy states of the well.

#### V. CONCLUDING DISCUSSION

The present study offers an analytic approach to the understanding of exciton-polariton condensates, which we believe is a welcome complement to experiment and numerical simulations. Our computations analytically demonstrate stationary solitons, and the prediction of a discontinuous band of dark solitons demonstrates a limitation of the single-field Gross-Pitaevskii model.

We have presented a detailed study of dark polariton soliton solutions of a system of equations for strongly coupled excitons and photons in the lossless case. One type of dark soliton studied is of the standard type where the fields vanish at the soliton center. This corresponds to complete depletion of the condensate at that point. In the positive detuning case, we have also reported a discontinuous soliton where the exciton field exhibits a jump at the soliton center, so the exciton density does not

vanish. We have shown that these two types of soliton can be unified in one branch, joined at the frequency where the discontinuity in the exciton density smoothly increases from zero.

The discontinuity of the soliton profile should not be considered unnatural. It is the result of neglecting the small excitonic dispersion, an approximation that provides a lot of calculational simplicity without compromising the phenomenology. If the excitonic dispersion is taken into account the jump discontinuity is replaced by a steep front. Integrability persists in this more precise calculation.

The solitons that we derive apply for a time interval after the pumping is removed and while the losses have not yet been significantly manifested or the solitons lie outside the pump spot. For example, in Refs. [6, 10] quasi-one-dimensional structures are observed outside the pump spots. This suggests that the rate of attenuation can be slow enough to allow for the formation of solitons, thus making the zero-loss assumption reasonable. The possibility to emulate lossless exciton-polaritons with a photonic system has been proposed [9], and a dark soliton is computed analytically for that system. In a different realization, polariton condensates can be created at two pump spots [17] and localized structures can be sustained in the region between the two spots where there is no pumping.

Coupled systems with nonlinearities serve as models for systems with two kinds of interacting particles when at least one of them is treated in a mean field description. They elucidate phenomena such as conservative soliton structures in an atomic condensate interacting with light [22] or vortex patterns in condensates with two atomic species [23]. The analysis in this article elucidates a nonlinear phenomenon that relies crucially on the coupling of

two systems: While one field is continuous and vanishes at a point of symmetry, the other may develop a discontinuous phase, thus allowing the associated density to remain strictly positive everywhere.

The solitons that we calculate are standing structures; they have zero velocity. They arise from the model equations by an exact calculation which is possible because the system can be integrated. Apparently they are the static members of families of traveling solitons. The calculation of traveling solitons would provide information on the dynamical behavior of polaritonic systems, particularly on the survival of discontinuous solitons. These calculations entail a significant broadening of the scope of the present work. The analytical challenge is to extract such solitons from a system of ordinary differential equations that is considerably more complicated than the integrable system that describes stationary solitons.

Polariton condensates emerge as a fertile ground for solitonic structures. Our results provide an analytic understanding of these structures and can lead to more accurate methods to describe dynamical behavior in polaritonic systems. For example, losses could be included within the framework of a perturbation theory on the conservative model.

This work was partially supported by the European Union's FP7-REGPOT-2009-1 project "Archimedes Center for Modeling, Analysis and Computation" (grant agreement n. 245749), by the (US) National Science Foundation under grants NSF DMS-0707488 and NSF DMS-1211638, and by EU and Greek national funds through the Operational Program "Education and Lifelong Learning"—THALES. This work has benefited from discussions with P. Savvidis, G. Christmann, F. Marchetti, G. Kavoulakis, A. Gorbach.

- 
- [1] A. V. Kavokin, J. J. Baumberg, G. Malpuech, and F. P. Laussy, *Microcavities* (Oxford University Press, New York, 2007).
  - [2] I. Carusotto and C. Ciuti, *Rev. Mod. Phys.* **85**, 299 (2013).
  - [3] H. Deng, H. Haug, and Y. Yamamoto, *Rev. Mod. Phys.* **82**, 1489 (2010).
  - [4] J. Keeling, F. M. Marchetti, M. H. Szymanska, and P. B. Littlewood, *Semiconductor Science and Technology* **22**, R1 (2007).
  - [5] Y. Larionova, W. Stolz, and C. O. Weiss, *Opt. Lett.* **33**, 321 (2008).
  - [6] A. Amo, S. Pigeon, D. Sanvitto, V. G. Sala, R. Hivet, I. Carusotto, F. Pisanello, G. Leménager, R. Houdré, E. Giacobino, C. Ciuti, and A. Bramati, *Science* **332**, 1167 (2011).
  - [7] S. Pigeon, I. Carusotto, and C. Ciuti, *Phys. Rev. B* **83**, 144513 (2011).
  - [8] R. Hivet, H. Flayac, D. D. Solnyshkov, D. Tanese, T. Boulier, D. Andreoli, E. Giacobino, J. Bloch, A. Bramati, G. Malpuech, and A. Amo, *Nat. Phys.* **8**, 724–728 (2012).
  - [9] L. Salasnich, B. Malomed, and F. Toigo, *Phys. Rev. E*, (2014)
  - [10] G. Grosso, G. Nardin, F. Morier-Genoud, Y. Léger, and B. Deveaud-Plédran, *Phys. Rev. B* **86**, 020509 (2012).
  - [11] M. Sich, D. N. Krizhanovskii, M. S. Skolnick, A. V. Gorbach, R. Hartley, D. V. Skryabin, E. A. Cerda-Méndez, K. Biermann, H. R., and S. P. V., *Nature Photonics* **6**, 50 (2012).
  - [12] O. A. Egorov, D. V. Skryabin, A. V. Yulin, and F. Lederer, *Phys. Rev. Lett.* **102**, 153904 (2009).
  - [13] O. A. Egorov, A. V. Gorbach, F. Lederer, and D. V. Skryabin, *Phys. Rev. Lett.* **105**, 073903 (2010).
  - [14] F. M. Marchetti and M. H. Szymanska, in *Exciton Polaritons in Microcavities: New Frontiers*, Vol. 172 of *Springer Series in Solid-State Sciences*, edited by D. Sanvitto and V. Timofeev (Springer-Verlag, ADDRESS, 2012).
  - [15] G. Grosso, G. Nardin, F. Morier-Genoud, Y. Léger, and B. Deveaud-Plédran, *Phys. Rev. Lett.* **107**, 245301 (2011).
  - [16] T. Ackemann, W. J. Firth, and G.-L. Oppo, in *Advances In Atomic, Molecular, and Optical Physics*, edited by E.

- Arimondo, P. R. Berman, and C. C. Lin (Academic Press, ADDRESS, 2009), Vol. 57, pp. Ch. 6, 323–421.
- [17] G. Tosi, G. Christmann, N. G. Berloff, P. Tsotsis, T. Gao, Z. Hatzopoulos, G. P. Savvidis, and J. J. Baumberg, *Nat. Phys.* **8**, 190 (2012).
  - [18] A. Dreismann, P. Cristofolini, R. Balili, G. Christmann, F. Pinsker, N. G. Berloff, Z. Hatzopoulos, G. P. Savvidis, and J. J. Baumberg, preprint (2014).
  - [19] *The Physics of Semiconductor Microcavities*, edited by B. Deveaud (Wiley-VCH, Weinheim, 2007).
  - [20] I. Carusotto and C. Ciuti, *Phys. Rev. Lett.* **93**, 166401 (2004).
  - [21] A. V. Yulin, O. A. Egorov, F. Lederer, and D. V. Skryabin, *Phys. Rev. A* **78**, 061801 (2008).
  - [22] M. Saffmann and D. Skryabin, in *Spatial Solitons*, edited by S. Trillo and W. Torruellas (Springer, Berlin Heidelberg, 2001), pp. Ch. 6, 433–447.
  - [23] R. Barnett, G. Rafael, M. A. Porter, and H. P. Büchler, *New J. Phys.* **10**, 043030 (2008).